



LED BASED LOW-COST PHOTO-ACOUSTIC SETUP BY USING STETHOSCOPE

Emine Ela DURMUŞ¹, Ensar KARABULUT¹, İbrahim AKKAYA^{2*}, Yavuz ÖZTÜRK²

¹Buca İnci-Özer Tırnaklı Science High School, 35678, Izmir, Türkiye


²Ege University, Department of Electrical and Electronics Engineering, 35100, Izmir, Türkiye


Abstract: In this study, design and characterization of a low-cost photo-acoustic setup is presented. Photo-acoustic effect is a very intriguing photo-thermo-acoustic effect having applications in a wide range from biomedical science to material characterization. The basic components of a photo-acoustic setup are a sound detector with or without an acoustic cell, a modulated light source preferably with enough power, and an absorbing object. One of the challenging problems is to couple the produced photo-acoustic waves into the detector and this problem was solved by using a commercial sound sensor module connected to a stethoscope. As a modulated light source simply a high power flashlight driven with an amplifier and MOSFET circuit was used. Both detection and light modulation were designed and operated to be via sound card input/output (I/O) of a computer and/or cell phone. Light power and frequency response of the system were presented and 523 Hz was determined as a resonance frequency of the system.


Keywords: Photo-acoustic, Low-cost, Stethoscope, Sound detection


*Corresponding author: Ege University, Department of Electrical and Electronics Engineering, 35100, Izmir, Türkiye

E mail: ibrahim-akkaya@hotmail.com (İ. AKKAYA)

Emine Ela DURMUŞ  <https://orcid.org/0000-0001-9910-0578>

Ensar KARABULUT  <https://orcid.org/0000-0001-7374-907X>

İbrahim AKKAYA  <https://orcid.org/0000-0003-0605-7115>

Yavuz ÖZTÜRK  <https://orcid.org/0000-0002-9650-6350>

Received: June 21, 2023

Accepted: August 22, 2023

Published: October 15, 2023

Cite as: Durmuş EE, Karabulut E, Akkaya İ, Öztürk Y. 2023. LED based low-cost photo-acoustic setup by using stethoscope. BSJ Eng Sci, 6(4): 369-374.

1. Introduction

Photoacoustic (PA) effect was discovered by Alexander Graham Bell in 1880, while he was experimenting with sound transport with light (Bell, 1880). At the same time period, similar PA experiments were done with liquids and gasses by the famous scientists John Tyndall and Wilhelm Röntgen as well. (Tyndall, 1880; Röntgen, 1881). Following that, from 1880 up to date, PA has been studied intensely in gas, liquid, and solid materials research. Furthermore, PA found applications in many different fields such as chemical energy estimation in chemistry (Malkin and Canaani, 1994), light intensity measurement in optics (Perelta et al., 1988; Aldama-Reyna et al., 2018), PA imaging in biomedical and medicine (Lucero and Chan, 2021), plant investigations in agriculture (Hernández-Aguilar C et al., 2008; Velasco et al., 2011; Singhal et al., 2022), bread characterization in food science (Hernández-Aguilar et al., 2021), painting investigations in art (Tserevelakis et al., 2017) and so on. The origin of the PA effect is the thermal effects due to the absorption of modulated continuous or pulsed light. These thermal effects can be in the form of thermal expansion or contraction and thermal diffusion (Rosencwaig and Gersho, 1976; Rousset et al., 1983). Both these outcomes produce pressure changes on the material and so acoustic waves. Many different systems have been developed to measure these acoustic waves. These systems in general have a light source to create

thermal effects, a sound detection device, and a PA measurement cell where the light energy transforms to heat and/or pressure waves. A PA cell has been generally designed and used for gas or liquid measurements, where the sample and sound detection device are separated by channels or placed in different configurations. However, in specific types of configurations for material research, the sample of interest is in contact with the sound detection unit which can be a piezoelectric sensor, or a microphone (Somer et al., 2013). In contact systems, acoustic waves need to be transferred into the sensor. Therefore, transferring the acoustic waves efficiently into the electrical or optical microphone is crucial. The majority of the studies about PA were conducted to optimize this transfer process (Sim et al., 2017). In many cases, determining the resonance frequency is very crucial to increase the signal to noise ratio (SNR) level (Sim et al., 2017).

The sound sensor structures used in previous studies are microphones based on capacitive, piezoelectric or optical. Many of these studies use custom acoustic cells and expensive sensor arrays. Several studies focused on low-cost light sources to reduce cost in PA experiments (Zhong et al., 2018). The paper, which inspired our study as well, using an easy access stethoscope showed the possibility of sound transfer via PA for educational purposes (Nikitichev et al., 2016).

In this study, an audible photoacoustic experimental



setup built with relatively low-cost and easy to find commercially available parts is presented. The system has an amplifier and modulation circuit to modulate an LED light source and a computer audio interface used to collect data from a sound sensor coupled to a stethoscope. All-important circuit characteristics are presented, a basic black vinyl tape is used as a sample and the resonance frequency of the system determined.

2. Materials and Methods

Optically generated acoustic waves due to the conversion of absorbed electromagnetic radiation energy to heat and pressure change is called photo-acoustic (PA) (Ma et al., 2020). There are two mechanisms formulated for PA as thermal diffusion and thermos-elastic bending (Rosencwaig and Gersho, 1976; Rousset et al., 1983; Mansanares et al., 1991; Somer et al., 2013). In thermo-elastic bending, thermal shape deformation is mainly caused by thermal expansion and/or contraction due to the temperature variation in the matter as shown in Figure 1. In thermal diffusion, the light absorbed in each cycle of the modulated light transforms to heat and propagates into the surrounding gas and produces temperature gradient along the direction of the surface normal.

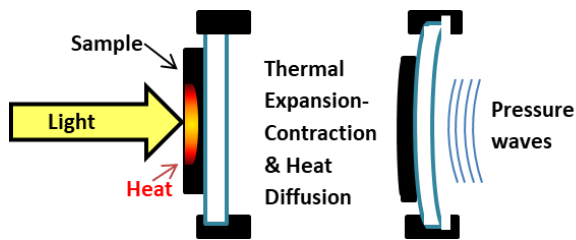


Figure 1. Mechanism of photoacoustic wave formation.

As mentioned earlier, the absorbed light energy is the source of the PA effect. This energy depends on the duration and absorbed power of the light (Rosencwaig and Gersho, 1976; Rousset et al., 1983). Therefore, PA signal amplitude is simply expected to be inversely proportional to the modulation frequency and proportional to the light power if a modulated continuous wave light is used as a source and it can be expressed as given in Equation 1 (Somer et al., 2013).

$$V_{pa}(f) = k_1(f) \frac{P}{f} + k_2(f) \frac{P}{f^{3/2}} + C \quad (1)$$

In here, P is the absorbed optical power, f is the modulation frequency of light, and $k_1(f)$ and $k_2(f)$ functions which depend on all the thermal, optical, and elastic properties of the absorbing material, ambient conditions, and the modulation frequency dependence of the electronic and mechanical system elements (Rosencwaig and Gersho, 1976; Rousset et al., 1983; Somer et al., 2013; Sim et al., 2017). In the PA detection, by measuring the $k_1(f)$ and $k_2(f)$ it is possible to

determine which mechanism is dominant between the thermal diffusion and thermos-elastic bending, respectively. C is a frequency invariant, constant value of a photoacoustic signal when there is no light excitation. For detailed information the theoretical studies can be read in the ref. Somer et al., (2013). In Equation (1), the term P/f is proportional to the energy of the incident light beam on the sample during each period of square wave modulated light. Therefore, if k is taken as a constant, it is expected to observe PA signal intensity decrease with ascending frequency.

2.1 Experimental Setup

The schematic of the designed system is given in Figure 2. The system consists of an amplifier circuit, white LED flashlight, spherical lens, stethoscope coupled by a sound sensor, computer, and a cell phone. First, to be able to obtain modulated light, an amplifier circuit was built by making some modifications based on the study of Nikitichev et al. (2013). An earphone jack was used to provide constant amplitude and variable sinusoidal frequency signals from a cell phone audio output to the amplifier circuit. Then, the amplifier circuit was directly connected to the voltage input of the light source. The projected light beams from the LED focused on to the stethoscope via the lens of the flashlight and an external lens with focal length +50 mm. A simple photodiode circuit was used to monitor the output of the light source. The photodiode was placed just in front of the light source not to prevent light from the flashlight to the stethoscope and stray light measured. The stethoscope was connected with its tube (length of 105 mm) to the sound sensor (KY-038, Joy-it, Germany). The microphone of the sound sensor was placed in the open end of the tube. The sound sensor was then connected to a computer via the microphone input port. An oscilloscope software (Soundcard Oscilloscope, Zeitnitz, Germany) was used to filter and measure the signals from the microphone unit.

The schematic of the amplifier and photodiode circuit is shown in Figure 3. The cell phone was connected to the amplifier circuit via an audio jack (3.5 mm stereo audio plug terminal block). The following high pass RC circuit ($R=75 \text{ k}\Omega$ and $C=100 \text{ nF}$), whose cutoff frequency was $\sim 150 \text{ Hz}$, used to suppress a possible DC bias of the input signal and also to filter out the network noise 50 Hz and its 2nd and 3rd harmonics due to the possible laboratory environment. If the 50 Hz network noise would be smaller, the high pass filter cutoff frequency may decrease $\sim 15 \text{ Hz}$. V_{ipp} and V_{opp} are peak-to-peak voltages of V_i and V_o , input and output amplifier voltages, respectively. The amplifier circuit designed to have gain ($G=V_{opp}/V_{ipp}$) of ~ 5 at higher frequencies than the cutoff. Also this circuit was designed to add a DC bias voltage around 3.9 V to the output of the amplifier. This DC Bias voltage can be adjusted to drive MOSFET on when there is no input voltage.

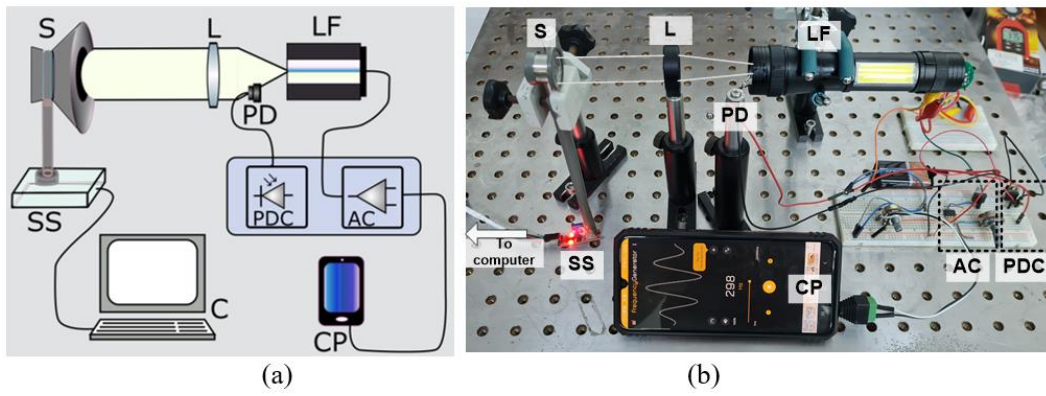


Figure 2. The experimental system design. (a) Schematic and, (b) actual view of the proposed system. AC: Amplifier circuit; C: Computer; CP: Cell phone. L: Lens; LF: LED flashlight; PD: Photodiode; PDC: Photodiode circuit; S: Stethoscope; SS: sound sensor.

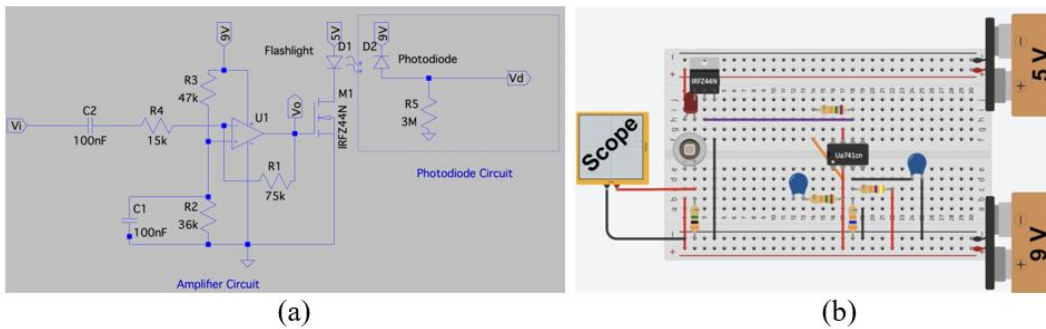


Figure 3. The proposed electrical circuit design of the amplifier and the photodiode. (a) analog circuit design and (b) the experimental design view on the breadboard.

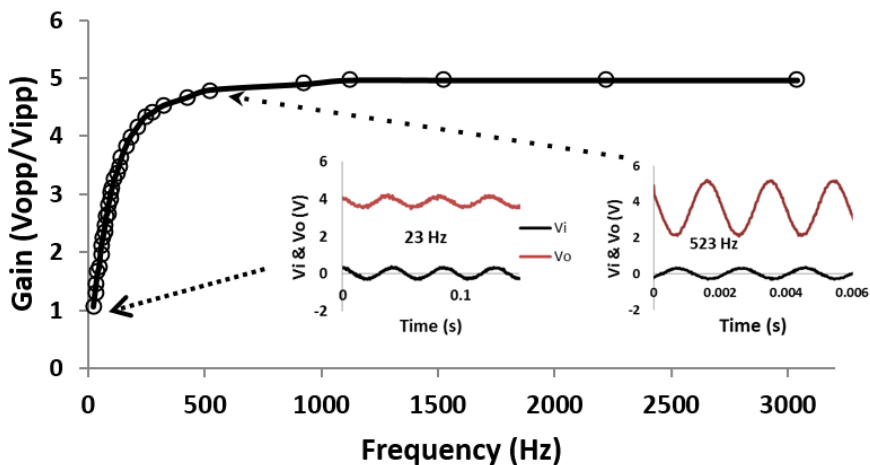


Figure 4. Gain changes against the frequency. V_{ipp} : amplifier input peak to peak voltage, V_{opp} : amplifier output peak to peak voltage.

The output of the amplifier circuit was connected to the gate pin of the MOSFET (Irfz44n, Transys Electronics, UK) to modulate the LED voltage connected to another 5 V source. V_i , V_o , and V_d voltages, monitored with the oscilloscope (GDS-2062, GW Instek, Taiwan), are all shown in Figure 3.

Although, the voltage output of the computer to the standard earphone (headphone) is expected to be $\sim 0.77 V_{RMS}$ ($2.2 V_{pp}$), the voltage range of the cell phone we used measured as $\sim 0.6 V_{pp}$. We first measured the input and output of the amplifier circuit. The average DC was 3.83

$\pm 0.1 V$ and a frequency dependent AC voltage (V_o) was observed. The ratio of input and output peak to peak voltages (V_{opp}/V_{ipp}) plotted with respect to frequency in Figure 4. The record of the oscilloscope voltages of V_i and V_o at the frequency of 23 Hz and 523 Hz is given in insets. A 3.83 V DC bias voltage was sufficient to activate the MOSFET. It is possible to adjust the on and off states duration of the MOSFET according to the transistor type and 36 and 46 k Ω resistors in the given circuit.

As an important parameter, the light output of the LED flashlight which indirectly determines the energy

absorbed by the material during excitation was measured by a photodiode shown in Figure 2. Since the flashlight was a white LED, it was arduous to measure and determine its intensity. We instead measured the light output with a lux-meter to give an idea about the light intensity. The focused non-modulated (continuous) light after the lens was first measured as 5660 Lux with an inexpensive lux-meter (UT-383, Uni-T, China). The photodiode circuit peak-to-peak voltage (V_{dpp}) was ~ 1.8 V during the constant, non-modulated light measurement. This value can give an idea about light intensity illuminating on the sample which was assumed to be proportional to the V_d voltage during the measurement of PA signal. The photodiode voltage was monitored with the oscilloscope and results of V_{dpp} presented in Figure 5, also voltage variations V_o and V_d at 523 Hz were presented in insets. The duty cycle of measured V_d was between $\sim 42\%$ and 44% in all measured frequency ranges. As can be seen from Figure 5, the gain G and DC bias values affect output of MOSFET and light modulation as well. Beyond around 150 Hz, the output of the light source was a square wave.

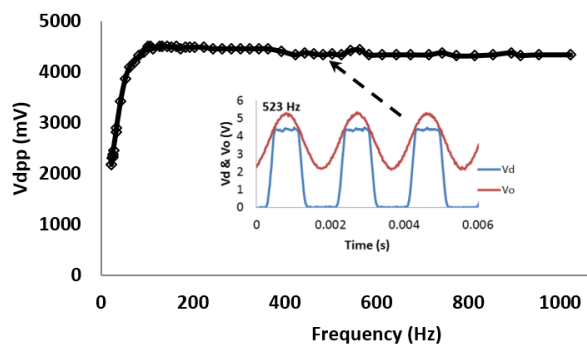


Figure 5. Photodiode circuit voltage V_{dpp} against frequency graph.

The system was built by easy to find commercial materials and components. The total cost of the system was around \$50 which is a relatively lower cost compared to other systems (Somer et al., 2013; Nikitichev et al., 2016, Zhong et al., 2018).

3. Results and Discussion

After building the experimental setup, a polyvinyl chloride (PVC) black tape was placed onto the stethoscope. During the measurements, photodiode voltage was monitored with the oscilloscope. The input voltage was set around $0.6 V_{pp}$. The created PA waves due to modulated light intensity variation on the stethoscope - sample surface was transferred to the used tube and then microphone. The electrical signal transferred into the computer microphone input was monitored and measured by soundcard oscilloscope software. A digital bandpass filter whose bandwidth was 2 Hz was applied by using the Soundcard Oscilloscope software. The filter type and order was Butterworth and 10, respectively. The mean PA signal voltage (V_{pa}) deviation was ± 0.1 mV

at a frequency range of 23 Hz to 1023 Hz. The measured V_{pa} values are shown in Figure 6. As it is seen from Eq. 1, V_{pa} is proportional to absorbed energy and light power, also inversely proportional to frequency. Additionally, V_{dpp} is proportional to light power. Therefore, V_{pa}/V_{dpp} ratio is related to V_{pa}/P . When we take the $k_1(f)$ and $k_2(f)$ values constant in Eq. 3, the ratio is inverse. However, when we acquire the resonance conditions, V_{pa}/V_{dpp} value will be higher (Rosencwaig and Gersho, 1976; Rousset et al., 1983). In Figure 6, the discrete line shows the theoretical curve which is proportional to $1/f$ and this curve overlaps with our experimental results besides the resonance interval. The PA signal can be modeled in two cases. One of them is thermal diffusion which is proportional to $1/f$, and the other one is thermoelastic bending is related to $1/f^{1.5}$ (Rosencwaig and Gersho, 1976; Rousset et al., 1983; Somer et al., 2013; Sim et al., 2017). When the PA signal is proportional to $1/f$, it means thermal diffusion mechanism is dominant (Mansanares et al.; 1998; Somer et al., 2013). The experimentally recorded signals acquired through thermally thick PVC tape. The similar results were acquired with the study in Ref Mansanares et al. (1998). In addition, the V_{pa} values from ~ 740 Hz and beyond are similar with no input light voltage value which is 0.03 ± 0.02 mV and we can call it dark voltage. Therefore, the dark voltage value was seen in the graph. One of the important findings was that the system was in resonance at 523 Hz. During measurements harmonics of the resonance frequency, with smaller amplitudes, were observed, but they did not be presented for the sake of simplicity. To make any measurements at resonance frequency 523 Hz, a higher signal to noise ratio (SNR) will be acquired than the other frequencies (Sim et al., 2017).

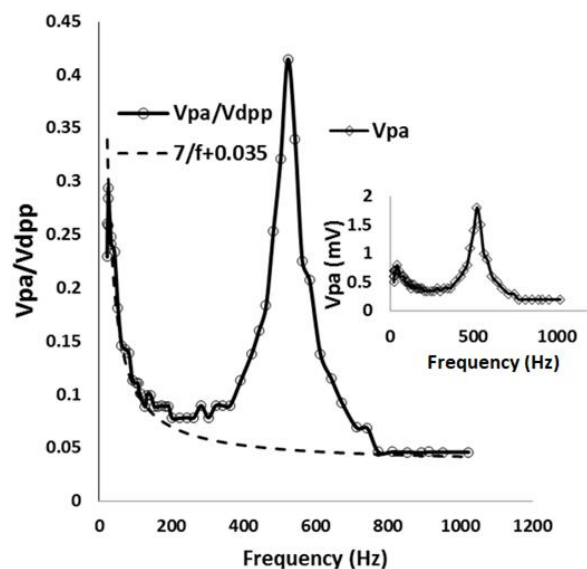


Figure 6. PA over detected light signal against frequency graph representation. Dotted line: theoretical, solid line: experimental.

After determination of the resonance frequency, $V_{dc}=5$ V voltage, given in Figure 3, changed to V_{dpp} values between 0.25 to 7.5 V via a DC power supply. V_{dpp} minimum voltage value was close to zero during all the measurements. Due to the fact that the V_{dpp} value is proportional to light power P, it shows the light power implicitly. Therefore, light power and V_{pa} are correlated with each other. Figure 7 shows this linear correlation between the light power (V_{dpp}) and V_{pa} . The outcomes are in-line with other studies in the literature where PA effect used as optical powermeter (Perelta et al., 1988; Inan et al., 2019; Ayoub et al., 2021).

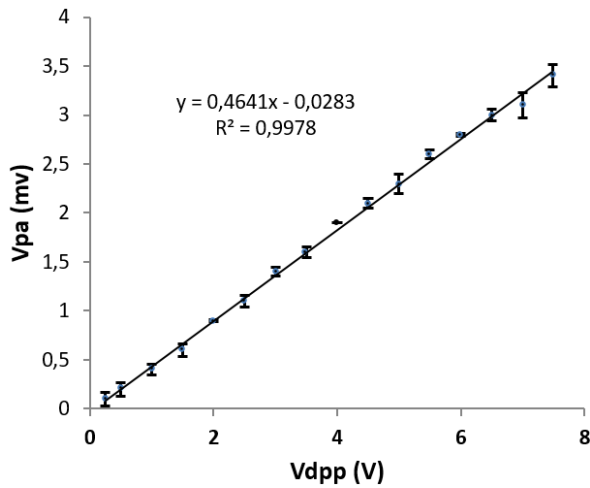


Figure 7. The correlation between the light source power and photoacoustic signal voltage.

In this research, the resonance frequency of the system was determined; the inverse relation between PA signal and modulation frequency and linear relation with the light power was shown as given in Equation 1.

4. Conclusion

In this study, a simple and low cost experimental setup was built from off the shelf components. Then, the photoacoustic (PA) effect and important parameters of this effect were given. Starting from the designed circuit, all the steps from electrical signals to optical signals within modulated in time, to acoustic waves, and then to the electrical signals again, and finally monitoring in the computer are shown. It is demonstrated that the measured PA signal by using a computer sound card as an oscilloscope is inversely proportional to light frequency and linearly proportional to light power. Furthermore, one of the important parameters for the measurements, the resonance frequency of the system was found at 523 Hz. The proposed study is considered to contribute to the photoacoustic field in research laboratory experiments and for preparing demonstrations. In addition, the proposed work is a multidisciplinary study which gathers optics, acoustics, mechanics, and electrical subjects, therefore; we believe that many undergraduate and graduate students and also researchers will favor their studies.

Author Contributions

The percentage of the author(s) contributions is presented below. All authors reviewed and approved the final version of the manuscript.

	E.E.D.	E.K.	İ.A.	Y.Ö.
C	20	20	30	30
D	30	30	20	20
S	15	15	25	45
DCP	30	30	20	20
DAI	30	30	20	20
L	30	30	20	20
W	25	25	30	20
CR	25	25	30	20
SR	10	10	70	10
PM	25	25	30	20

C=Concept, D= design, S= supervision, DCP= data collection and/or processing, DAI= data analysis and/or interpretation, L= literature search, W= writing, CR= critical review, SR= submission and revision, PM= project management, FA= funding acquisition.

Conflict of Interest

The authors declared that there is no conflict of interest.

Ethical Consideration

Ethics committee approval was not required for this study because of there was no study on animals or humans.

References

- Aldama-Reyna CW, Aldama-Guardia JD, Agreda-Delgado JF. 2018. Infrared laser pulse energy detector based on photoacoustic effect. *Momento-Revista De Fisica*, 56: 87-103.
- Ayoub HS, El-Sherif AF, Maize SM, Elbasha YH. 2021. Design and implementation of photoacoustic based beam dump-average optical power meter for fast and ultrafast lasers. *Opt Lasers Eng*, 140: 106548.
- Bell AG. 1880. On the production and reproduction of sound by light. *American J Sci*, 118: 305-324.
- Hernández-Aguilar C, Mezzalama M, Lozano N, Cruz-Orea A, Martínez E, Ivanov R, Domínguez-Pacheco A. 2008. Optical absorption coefficient of laser irradiated wheat seeds determined by photoacoustic spectroscopy. *The European Physical J Special Top*, 153(1): 519-522.
- Hernandez-Aguilar C, Dominguez-Pacheco A, Valderrama-Bravo C, Cruz-Orea A, Ortiz E M, Ivanov, R, Ordóñez-Miranda J. 2021. Photoacoustic characterization of wheat bread mixed with *Moringa oleifera*. *Curr Res Food Sci*, 4: 521-531.
- Inan I, Öztürk Y, Özdemir İE. 2019. Optical power measurement by using piezo microphone. In: *Innovations in Intelligent Systems and Applications Conference (IASIU)*, Oct. 31 – Nov. 02, 2019, Izmir, Türkiye, pp: 1-4.
- Lucero MY, Chan J. 2021. Photoacoustic imaging of elevated glutathione in models of lung cancer for companion diagnostic applications. *Nature Chem*, 13(12): 1248-1256.
- Ma Y, Qiao S, Patimisco P, Sampaolo A, Wang Y, Tittel FK, Spagnolo V. 2020. In-plane quartz-enhanced photoacoustic spectroscopy. *Appl Physics Lett*, 116(6): 061101.
- Malkin S, Canaani O. 1994. The use and characteristics of the photoacoustic method in the study of photosynthesis. *Ann Rev Plant Physiol Plant Molec Biol*, 45(1): 493-526.

- Mansanares AM, Vargas H. 1991. Photoacoustic characterization of a two-layer system. *J Appl Physics*, 70: 7046.
- Nikitichev DI, Xia W, Hill E, Mosse CA, Perkins T, Konyn K, Ourselin S, Desjardins AE, Vercauteren T. 2016. Music-of-light stethoscope: a demonstration of the photoacoustic effect. *Phys Educ*, 51: 045015.
- Perelta SB, Al-Khafaji HH, Williams AW. 1988. Photoacoustic optical power meter using piezoelectric detection. *J Physics E: Sci Instrum*, 21(2): 195.
- Röntgen WC. 1881. On tones produced by the intermittent irradiation of a gas. *Philos Mag Lett* 5, 11(68): 308-311.
- Rosencwaig A, Gersho A. 1976. Theory of the photoacoustic effect with solids. *J Appl Physics*, 47(1): 64-69.
- Rousset G, Lepoutre F, Bertrand L. 1983. Influence of thermoelastic bending on photoacoustic experiments related to measurements of thermal diffusivity of metals. *J Appl Physics*, 54(5): 2383-2391.
- Sim JY, Ahn CG, Huh C, Chung KH, Jeong EJ, Kim BK. 2017. Synergetic resonance matching of a microphone and a photoacoustic cell. *Sensors*, 17(4): 804.
- Singhal SK, Singh KP, Joshi SK, Rai AK. 2002. Diagnosis and study of fungal diseases of wheat by photoacoustic spectroscopy. *Curr Sci*, 82(5): 172-176.
- Somer A, Camilotti F, Costa G F, Bonardi C, Novatski A, Andrade AVC, Kozlowski Jr VA, Cruz GK. 2013. The thermoelastic bending and thermal diffusion processes influence on photoacoustic signal generation using open photoacoustic cell technique. *J Appl Physics*, 114: 063503.
- Tserevelakis GJ, Vrouvaki I, Siozos P, Melessanaki K, Hatzigiannakis K, Fotakis C, Zacharakis G. 2017. Photoacoustic imaging reveals hidden underdrawings in paintings. *Sci Rep*, 7(1): 1-11.
- Tyndall J. 1880. Action of an Intermittent Beam of Radiant Heat upon Gaseous Matter. *Proc Royal Soc London*, 31: 307-317.
- Velasco DS, Baesso ML, Medina AN, Bicanic DD, Koehorst R, van der Hooft JJJ, Bento AC. 2011. Thermal diffusivity of periderm from tomatoes of different maturity stages as determined by the concept of the frequency-domain open photoacoustic cell. *J Appl Physics*, 109(3): 034703.
- Zhong H, Duan T, Lan H, Zhou M, Gao F. 2018. Review of low-cost photoacoustic sensing and imaging based on laser diode and light-emitting diode. *Sensors*, 18(7): 2264.